NASA/CR-2000-210118
ICASE Report No. 2000-22

Simultaneous Velocimetry and Thermometry of Air Using Nonresonant Heterodyned Laser-induced Thermal Acoustics

Roger C. Hart
ICASE, Hampton, Virginia

R. Jeffrey Balla and G.C. Herring
NASA Langley Research Center, Hampton, Virginia

Institute for Computer Applications in Science and Engineering
NASA Langley Research Center
Hampton, VA

Operated by Universities Space Research Association

National Aeronautics and
Space Administration

Langley Research Center
Hampton, Virginia 23681-2199

Prepared for Langley Research Center
under Contract NAS1-97046

May 2000

SIMULTANEOUS VELOCIMETRY AND THERMOMETRY OF AIR USING NONRESONANT HETERODYNED LASER-INDUCED THERMAL ACOUSTICS

ROGER C. HART[1], R. JEFFREY BALLA[2], AND G. C. HERRING[2]

Abstract. Non-resonant laser-induced thermal acoustics (LITA) is employed with heterodyne detection to measure temperature (285-295 K) and a single component of velocity (20-150 m/s) in an atmospheric pressure, subsonic, unseeded air jet. Good agreement is found with pitot-tube measurements of velocity (0.2% at 150 m/s and 2% at 20 m/s) and the isentropic expansion model for temperature (0.3%).

Key words. velocimetry, thermometry, heterodyne, nonresonant Light Scattering, laser-induced thermal acoustics, LITA

Subject classification. Physical Sciences

1. Introduction. Non-intrusive optical velocimetry is done either by intervalometry (e.g., particle image velocimetry or cross-correlation techniques) or by observing the Doppler shift $\Delta\omega$. Examples of the second approach are laser Doppler velocimetry (LDV) and planar Doppler velocimetry (PDV). Accurate measurement of the small Doppler shift found in typical subsonic aerodynamic applications is challenging. In PDV differential transmission at the absorption edge of an atomic line filter provides the necessary frequency resolution. With LDV, what is essentially a heterodyne technique is used. Both of these approaches require seeding with small particles. Seeding is inconvenient in some instances and impossible in others. Potential seeding problems include nonuniformities in the seed density, pitting of smooth model surfaces, seed particles lagging the flow, and the inability to seed specific locations (e.g., boundary layer).

Laser-induced thermal acoustics (LITA) is a seedless diagnostic technique in which optical interference patterns induce sound waves and thermal gratings in the medium. Early gas-phase work [1-3] utilized a resonant version of LITA, in which the pump laser frequency was resonant with a molecular transition. Absorption in the molecule of interest, followed by thermalization, generated a stationary thermal grating and two moving acoustic gratings. These gratings were used to demonstrate sound speed measurements [4] versus pressure. More recently, nonresonant versions have been demonstrated for thermometry [5-7] and sound speed measurements [8] versus temperature. The nonresonant version generates only two moving acoustic gratings. Because nonresonant LITA does not require absorption, it is convenient for interrogation of a variety of atomic and molecular species. Hence, non-resonant LITA is attractive for application to a wide array of wind tunnels using various test gases. Most recently

[1] Institute for Computer Applications in Science and Engineering (ICASE), NASA Langley Research Center, Hampton, VA 23681-2199. This research was supported by the National Aeronautics and Space Administration under NASA Contract No. NAS1-97046 while the first author was in residence at the Institute for Computer Applications in Science and Engineering (ICASE), NASA Langley Research Center, Hampton, VA 23681-2199.

[2] AMDB, NASA Langley Research Center, Hampton, VA 23681-2199.

heterodyned velocimetry [9] has been achieved with resonant LITA. In this letter, we demonstrate, simultaneously, heterodyned velocimetry and thermometry with nonresonant LITA at a single spatial point.

2. Description of Heterodyne LITA Velocimetry. In nonresonant LITA, two crossed beams from a short-pulse pump laser create counter-propagating acoustic plane wave packets in the medium by electrostriction. Illumination of these wave packets with a second long-pulse probe laser, at frequency Ω_L, generates a Bragg-diffracted signal beam that consists of two overlapped and co-propagating (but distinct) components. These two components are distinguished by their different Doppler shifts, $\pm \Delta\omega$, which are determined by the counter-propagating geometry of the two acoustic wave packets. The beating together of the two components, at frequencies $\Omega_L \pm \Delta\omega$, produces a modulation of this Bragg-diffracted signal beam at frequency $2\,\Delta\omega$. If the sound wave reciprocal wavelength is $\Delta\mathbf{k}$ (i.e., wave vector difference of the two pump beams) and bold-faced quantities denote vectors, the two Doppler shifts are $\Delta\omega = \Delta\mathbf{k} \bullet (\pm\mathbf{V}_S)$, where $\pm\mathbf{V}_S$ are the velocities of the two counter-propagating wave packets and $|\pm\mathbf{V}_S|$ = the speed of sound. Measurement of the beat frequency $2\,\Delta\omega$, with the known grating wavelength $1/\Delta\mathbf{k}$, yields the sound speed. Temperature T is also determined because $T \propto \sqrt{V_S}$. If the medium is in motion at velocity $\mathbf{V}_F$ (assumed to be parallel to $\Delta\mathbf{k}$ and $\mathbf{V}_S$) the frequencies of the signal beam are shifted to $\Omega_L + \Delta\mathbf{k} \bullet (\mathbf{V}_F \pm \mathbf{V}_S)$, but the difference frequency and the beating are unchanged.

The bulk fluid motion at velocity $\mathbf{V}_F$ is also readily obtained from LITA. Walker et al. [10], have demonstrated LITA velocimetry using a single-mode probe laser and etalon to detect the shift due to fluid flow in the frequency domain. Here we use an approach [11], which does not require a narrow band, frequency-stable probe source or a high-finesse etalon. We introduce a local oscillator beam at the probe frequency Ω_L, of suitable intensity, that is collinear with the diffracted signal beam. The detected signal then shows modulation at three frequencies: $2\,\Delta\omega$ and $\Delta\omega \pm (\Delta\mathbf{k} \bullet \mathbf{V}_F)$. The measured frequency at $2\,\Delta\omega$ again gives $\mathbf{V}_S$ and T, while $\mathbf{V}_F$ is found from the difference in frequency $2\,\Delta\omega'$ between the other two components, where $\Delta\omega' = \Delta\mathbf{k} \bullet \mathbf{V}_F$. The signal is digitized, and the frequencies are extracted either by spectral methods (Prony's method) or by Levenberg-Marquardt fitting in the time domain. Thus $V_S = \Delta\omega / \Delta k$, $T \propto \sqrt{V_S}$, and $V_F = V_S\,\Delta\omega' / \Delta\omega = \Delta\omega' / \Delta k$. Sound speed, temperature, and one component of fluid velocity are determined simultaneously in a measurement time of about 1 μs.

3. Experimental Apparatus. The experimental setup is shown in the schematic of Fig. 1. Two 7-ns pump pulses (532 nm) are derived from a single laser beam (not shown) and crossed at $2\,\theta = 0.9$ deg, making sure that longitudinal coherence between the two beams is maintained at the crossing point. The ~10 μs probe pulse (750 nm), derived from a second laser, traverses the crossing point at the Bragg phase-matching angle of $\phi = 0.6$ deg. Both lasers operate at 10 Hz, however LITA data is acquired at 1 Hz. Peak pulse intensities are about 7 MW and 3 kW for the pump and probe beams, respectively. A fraction of the 750-nm beam is split off (not shown) from the probe to use as the local oscillator (LO) beam, which is directed exactly along the path expected for the Bragg-diffracted LITA signal. A beam block for both of

the pumps and the probe reduces scattered light into the detector. The sample volume, defined by the overlap volume of the crossing of the probe and LO input beams, is ellipsoidal, about 1 by 15 mm, with the longer dimension collinear with the optic axis and perpendicular to the flow direction. The long axis of the ellipsoid is located 5 mm downstream from the exit plane of a subsonic jet. A variable-speed jet exhausting into the room air (with a 5 by 35-mm rectangular cross section nozzle) was used to produce a range of uniform flow velocities over the sample volume, by varying the backing pressure of the jet.

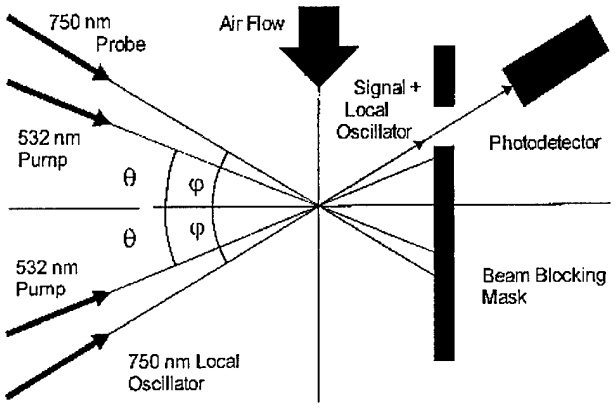

FIG. 1. *Schematic of the setup used to make temperature and heterodyned velocity measurements with LITA.*

A photomultiplier tube is used to monitor the time dependent signal intensity that results from both the Bragg-diffracted signal and the LO that propagate at angle ϕ through the aperture in the blocking mask of Fig. 1. The signals are digitized with 500-MHz-bandwidth oscilloscopes. As in Ref. [7], a second LITA signal is simultaneously generated in a reference cell with known temperature to use as a reference signal to normalize out small pulse-to-pulse fluctuations in the beam crossing angles. This normalizing correction improved the quality of data in [7], but turned out to be negligible compared to random errors in the current experiments.

A typical example of the digitized LITA signal (noisy curve) obtained for a single laser pulse with a nonzero flow velocity is shown in Fig. 2a. We first apply Prony's method to the data of Fig. 2a to determine the important frequency components. We use the result from Prony's method as the initial guess in a nonlinear least squares fitting routine. The result of this Levenberg-Marquardt fitting routine (smooth curve) is then taken as the final result for the values of the beat frequencies. The difference between the fit and the data (noisy curve) is shown (with the same scale as used for the upper trace) in the lower trace of Fig. 2a. Fig. 2b shows three peaks in the spectral transform of the temporal data of Fig. 2a. The value of 2 $\Delta\omega$ is given by the frequency of the right-most peak, while the value of 2 $\Delta\omega'$ is given by the frequency difference of the two left-most peaks. In the example of Fig. 2, the airflow speed is about 25 m/s.

With our geometry (the probe beam is larger than the pump beam at the crossing point), to obtain the degree of precision reported here, we have to include the motion of the density gratings in the model that we fit to the data. Because the detector is fixed, the propagation of small acoustic wave packets across the larger probe beam changes the scattering angle and the magnitude of the Doppler shift. In other words, there is a very small frequency chirp (not obvious to the eye in Fig. 2a, but detectable in the fitting) over the two microseconds that we observe the LITA signal. The differences between the fits and the data are significantly reduced, especially at low velocities, when we include this grating motion (or frequency chirp) in the fitting model.

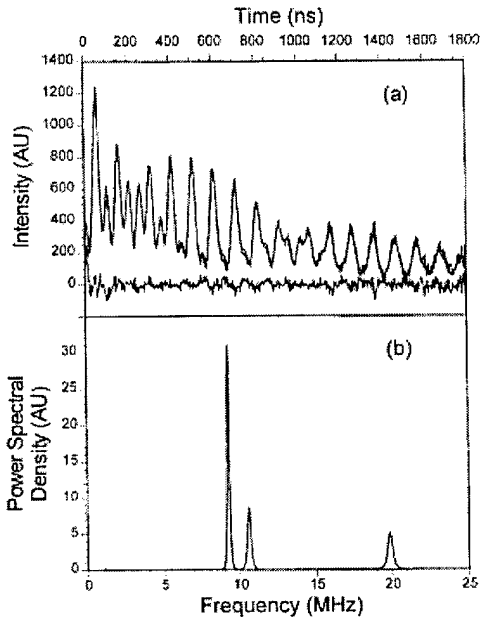

FIG. 2. *In the upper trace of (a), a single-laser-shot heterodyned LITA example of the temporal profile shows the data [noisy curve] and a fit to the data [smooth curve]. The lower trace of (a) shows the difference between the fit and the data. In (b) the corresponding spectral transform of the data is shown. Velocity, Mach number and temperature are obtained from the frequencies of the three peaks.*

4. Results. A comparison between LITA and pitot tube velocity measurements is shown in Fig. 3. In Fig. 3a, LITA velocity is plotted and, in Fig. 3b, the percentage difference ($100 * [V_{LITA} - V_{pitot}] / V_{pitot}$) is plotted - both versus pitot-tube velocity. Pitot-tube data is acquired simultaneously with the LITA data, but 4 mm downstream from the LITA measurement location (i.e., 9 mm downstream of the jet exit plane). Placing the LITA beams closer to the pitot tube would have scattered laser light that would have degraded the LITA signal-to-noise ratio. After blocking the LITA laser beams, we have measured the velocity gradient between these two measurement locations with the pitot tube. The magnitude of the velocity gradient, between the two measurement locations, was about 1-2% of the velocity at the low-end

(20 m/s) of the velocity range and about 10 times smaller at the high-end (150 m/s). The comparison between the LITA and pitot-tube measurements shown in Fig. 3 has been corrected for the velocity gradient between the 5 and 9-mm positions. The differences between LITA and pitot-tube measurements vary from 0.2% near 150 m/s to 2% near 20 m/s. Each LITA velocity and velocity difference data point shown is the average of about ~ 50 laser shots. Error bars are omitted for clarity. In part (a), one standard deviation of the population of the LITA data is about the size of the symbol. For the differences shown in part (b), one-standard deviation of the population for each averaged point varies from ± 1% at 150 m/s to ± 4% at 20 m/s. For both parts of Fig. 3, the errors in the mean values are about $\sqrt{50} \approx 7$ times smaller.

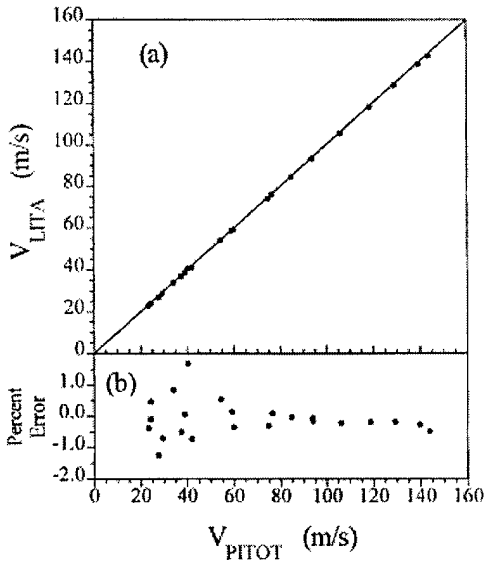

FIG. 3. *LITA (a) velocity and (b) the difference between LITA and a pitot tube versus the pitot-tube velocity. Pitot tube data are acquired simultaneously with the LITA data. Each velocity and velocity difference point is the average of ~ 50 laser shots.*

In Fig. 4a, LITA temperature (solid circles), for the same run as in Fig. 3, is plotted versus pitot-tube velocity, along with an isentropic flow calculation (open diamonds) that is based on the measured stagnation temperature inside the plenum of the flow generator and the measured pitot-tube Mach number. In Fig 4b, the percentage difference ($100 * [T_{LITA} - T_{calc}] / T_{calc}$) is plotted. The differences are 0.3% or less. Each temperature and difference data point shown is the average of ~ 50 laser shots. Error bars are also omitted from Fig. 4 for clarity. In part (a), one standard deviation of the population for each LITA data point is typically ± 1.1 K or ± 0.4%. Again, the one-standard deviations of the means are about $\sqrt{50} \approx 7$ times smaller.

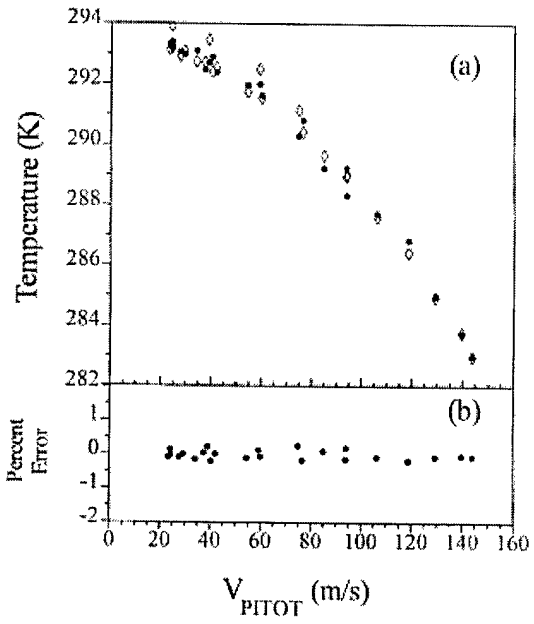

FIG. 4. *LITA (a) temperature measurements (solid circles) obtained from the same data set as used in Fig. 3, plotted as a function of pitot-tube velocity, and compared to an isentropic-flow calculation (open diamonds). The differences between LITA data and calculation are shown in (b).*

5. Conclusion. In summary, non-resonant LITA has been demonstrated with heterodyne detection to measure simultaneously temperature and a single component of velocity at a single point in a free-expansion atmospheric-pressure air jet. The agreement of the LITA velocity with simultaneous pitot-tube measurements varies from 0.2% at 150 m/s to 2% at 20 m/s. The LITA temperature measurements agree with the isentropic expansion model within about 0.3% for the temperature range 285-295 K. The good agreement between LITA and these established methods suggests that nonresonant LITA can be reliably used for simultaneous flow velocimetry and thermometry for these flow conditions.

Acknowledgements. We gratefully thank D. Morris (Kennedy Space Center) for contributing to this work.

REFERENCES

[1] S. WILLIAMS, L.A. RAHN, P.H. PAUL, J.W. FORSMAN, AND R.N. ZARE, *Laser-induced Thermal Grating Effects in Flames*, Opt. Lett. **19** (1994), pp. 1681-1683.

[2] E.B. CUMMINGS, *Laser-induced Thermal Acoustics: Simple Accurate Gas Measurements*, Opt, Lett. **19** (1994), pp. 1361-1363.

[3] M.A. BUNTINE, D.W. CHANDLER, AND C.C. HAYDEN, *Detection of Vibrational Overtone Excitation in Water Via Laser-Induced Grating Spectroscopy*, J. Chem. Phys. **102** (1995), pp. 2718-2726.

[4] E.B. CUMMINGS, H.G. HORNUNG, M.S. BROWN, AND P.A. DEBARBER, *Measurement of Gas-phase Sound Speed and Thermal Diffusivity Over a Broad Pressure Range Using Laser-induced Thermal Acoustics*, Opt. Lett. **20** (1995), pp. 1577-1579.

[5] A. STAMPANONI-PANARIELLO, B. HEMMERLING, AND W. HUBSCHMID, *Temperature Measurements in Gases Using Laser Induced Electrostrictive Gratings*, Appl. Phys. B **67** (1998), pp. 125-130.

[6] M.S. BROWN AND W.L. ROBERTS, *Single Point Thermometry in High-Pressure Sooting, Premixed Combustion Environments*, J. Propulsion Power **15** (1999), pp. 119-127.

[7] R.C. HART, R.J. BALLA, AND G.C. HERRING, *Nonresonant Referenced Laser-Induced Thermal Acoustics Thermometry in Air*, Appl. Opt. **38** (1999), pp. 577-584.

[8] R.C. HART, R.J. BALLA, AND G.C. HERRING, *Optical Measurement of the Speed of Sound in Air Over the Temperature Range 300-650 K*, J. Acoust. Soc. Am., accepted for publication.

[9] S. SCHLAMP, E.B. CUMMINGS, AND T.H. SOBOTA, *Laser-Induced Thermal-Acoustic Velocimetry With Heterodyne Detection*, Opt. Lett. **25** (2000), pp. 224-226.

[10] D.J.W. WALKER, R.B. WILLIAMS, AND P. EWART, *Thermal Grating Velocimetry*, Opt. Lett. **23** (1998), pp. 1316-1318.

[11] A.A. MAZNEV, K.A. NELSON, AND J.A. ROGERS, *Optical Heterodyne Detection of Laser-Induced Gratings*, Opt. Lett. **23** (1998), pp. 1319-1321.